within the experimental accuracy of our system. This means that the frequency change must be smaller than 25 MHz, so that it is justified to proceed with the constant-frequency assumption when using (1) for the determination of $g_d(v_{ac})$.

ACKNOWLEDGMENT

The authors wish to thank D. J. Colliver of the Royal Radar Establishment for his advice and help and for supplying the InP devices.

REFERENCES

[1] D. D. Khandelwal and W. R. Curtice, "A study of the single-frequency quenched-domain mode Gunn-effect oscillator," *IEEE Trans. Microwave Theory Tech.*, vol. MTT-18, pp. 178–187, Apr. 1970.
[2] M. Kawashima and H. Hartnagel, "New measurement method of Gunn-diode impedance," *Electron. Lett.*, vol. 8, p. 305, 1972.
[3] R. P. Owens and D. Cawsey, "Microwave equivalent-circuit parameters of Gunn-effect-device packages," *IEEE Trans. Microwave Theory Tech. (Special Issue on Microwave Circuit Aspects of Avalanche-Diode and Transferred Electron Devices)*, vol. MTT-18, pp. 790–798, Nov. 1970.
[4] J. C. Slater, *Microwave Electronics*. New York: Van Nostrand, 1950, p. 207.

An Experimental Study of Stabilized Transferred-Electron Amplifiers

ASHOK K. TALWAR AND WALTER R. CURTICE

***Abstract*—Experimental data are presented to describe various characteristics of stabilized transferred-electron amplifiers. The effect of bias voltage upon RF gain and linearity is shown. The conditions under which gain expansion is observed are described, and the importance of lattice temperature and RF signal strength in determining dc current is shown. All results are shown to be in good agreement with the large-signal theory for these amplifiers.**

INTRODUCTION

STABILIZED transferred-electron devices have been shown to be useful in obtaining broad bandwidth amplification at microwave frequencies [1], [2]. The devices and amplifiers are stable in the sense that RF oscillation does not occur when the input signal is removed. The observation of gain expansion [3] and unstable operation at certain values of bias voltage [1] have now been explained by a detailed large-signal analysis presented by Talwar [4] and Talwar and Curtice [5]. This paper summarizes the results of an experimental investigation of these effects and other experimental properties. It is shown that all properties are in agreement with the large-signal theory.

The method of theoretical analysis and some calculated characteristics of stabilized TE devices were presented by Talwar and Curtice [6] in 1971. It is assumed that the increased lattice temperature present in CW devices permits a stable electric field configuration to exist in the absence of external RF signals. Assuming specific external ac and dc current excitation, a set of one-dimensional large-signal differential equations is solved, progressing from the cathode contact. The effects of field-dependent diffusion are included as correction terms. Only dc and fundamental frequency RF electric fields are assumed to be important, whereas the effects of current harmonics are included. By integration of the electric field quantities over the total length of the device, the dc operating voltage and the RF impedance are obtained. The behavior of dc and RF impedance as functions of device parameters (including lattice temperature), operating bias, RF signal level, and RF signal frequency has been studied [4].

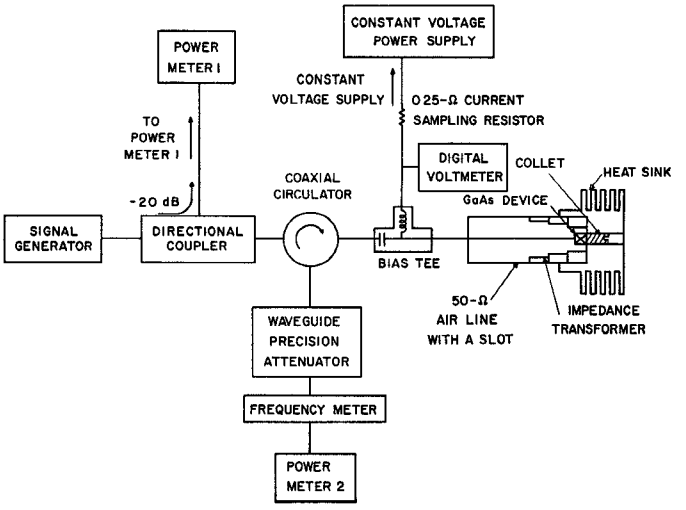

Fig. 1. Schematic diagram of the circuit used for the experimental study of stabilized TE amplifiers.

A. Description of the Circuit and the GaAs Diodes Used for the Experimental Study

A schematic diagram of the circuit used for most of the tests is shown in Fig. 1. The device is mounted in series with

Manuscript received November 6, 1972; revised February 26, 1973. This work was supported by the Air Force Systems Command, Rome Air Development Center, under Contract F30602-71-C-0099.

A. K. Talwar was with the Electron Physics Laboratory, Department of Electrical and Computer Engineering, University of Michigan, Ann Arbor, Mich. 48104. He is now with the Product Development Laboratories, Ford Motor Company, Dearborn, Mich. 48121.

W. R. Curtice was with the Electron Physics Laboratory, Department of Electrical and Computer Engineering, University of Michigan, Ann Arbor, Mich. 48104. He is now with the David Sarnoff Research Center, RCA Corporation, Princeton, N. J. 08540.

TABLE I
DEVICE PARAMETERS

Device	n_o(/cm^3)	l (μm)	Resistance at Low Bias (Ω)	Hall Mobility (cm^2/V·s)
1	1.0×10^{15}	11.0	5.8	6300
2	0.9×10^{15}	8.5	5.3	—
3	0.5×10^{15}	14.0	2.7	7060
4	0.5×10^{15}	14.0	2.7	7060
5	0.5×10^{15}	14.0	7.6	7060
6	0.5×10^{15}	14.0	7.0	7060

the center conductor at the end of a coaxial transmission line of 50-Ω characteristic impedance. A broad bandwidth coaxial circulator separates the input and output signals. All data are obtained using a constant voltage power supply and CW operation except for the pulsed current–voltage measurements. Reflection gain numbers will refer to the gain seen on the device side of the bias tee. Corrections for circuit loss were made by replacing the coaxial circuit and device by a short circuit. The input power to the amplifier was evaluated at the device side of the bias tee by allowing for the circuit loss from the directional coupler to the input of the coaxial circuit.

Movable tuning slugs of one-quarter wavelength (at 10 GHz) were used for the purpose of controlling the circuit impedance presented to the device. A slot in the transmission line allowed for the adjustment of the position of the slugs. Two Chebyshev transformers were made to transform the 50-Ω coaxial line impedance to 25 and 10 Ω, respectively. Each transformer had three slugs of length $\lambda/4$ at 10 GHz. The transformers were designed to have a bandwidth of approximately 7 GHz for the 25-Ω transformer and approximately 5 GHz for the 10-Ω transformer, allowing a maximum theoretical reflection coefficient (with a matched load) of 0.05 and 0.11, respectively.

The devices were all obtained from the Monsanto Company. They consist of encapsulated epitaxial $n\text{-}^+n\text{-}n^+$ chips (approximately 0.008 in square) mounted on the copper studs of the packages. The values of lead inductance and package capacitance given by the supplier are 0.46 nH and 0.26 pF, respectively. Some of the basic characteristics of the crystals are shown in Table I. The values of n_o, l, and mobility given in the table are provided by the manufacturer. The thermal resistance given by the supplier is 30° C/W. Devices 3, 4, 5, and 6 are from the same wafer.

Fig. 2 shows pulsed and CW bias currents as functions of bias voltage for device 2. The device was mounted in the 50-Ω line with the 10-Ω transformer placed at the device end. No oscillations were observed at any bias tested in this circuit. The pulsed characteristic is for a pulse width of 0.5 μs and a repetition rate of 1000 pps.

For the same bias voltage, the bias current is seen to be smaller for dc bias than when the device is operated with a pulsed bias. This difference (decrease) in current is directly due to an increase in the lattice temperature caused by the dc power dissipation. The current difference increases as bias voltage is increased because the lattice temperature (and dc power dissipation) increases. The CW current–voltage characteristic usually exhibits a maximum value of current close to but not exactly equal to the bias for which the threshold of Gunn effect is expected. Thus a current decrease occurs above threshold for stabilized CW devices without formation of high-field domains.

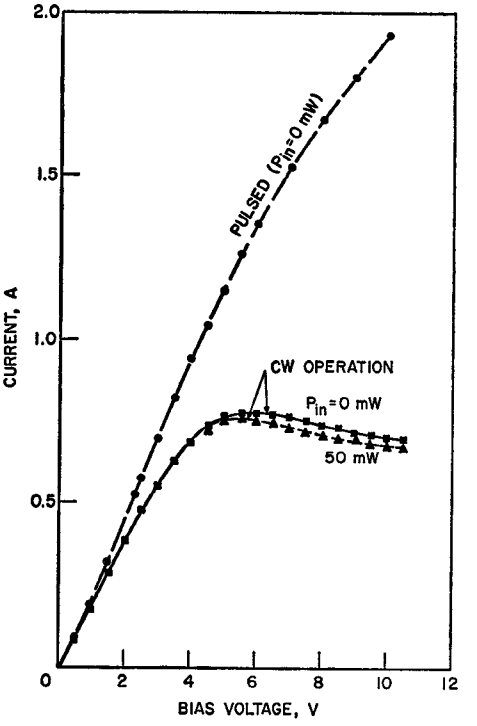

Fig. 2. Relationship between bias current and bias voltage for device 3 under pulsed and CW conditions. The 50-mW input power is at 8.8 GHz. The 10-Ω impedance transformer was used.

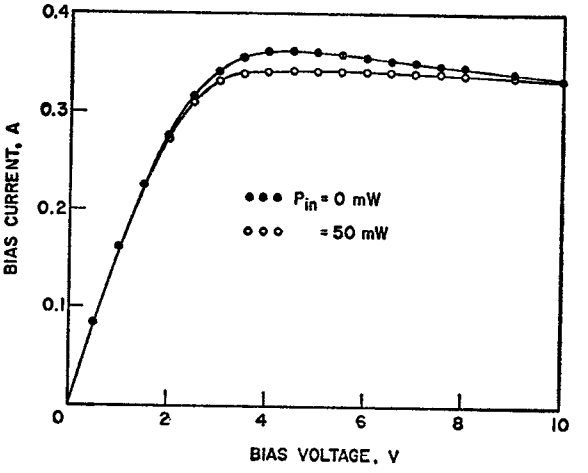

Fig. 3. CW current–voltage relationships for device 1. The 50-mW input power is at 10 GHz. The 25-Ω impedance transformer was used.

Talwar [4] shows that when a large signal is injected into a stabilized diode, the bias current will decrease if the diode is biased with a constant voltage supply. This is demonstrated in Fig. 2 where the CW current–voltage relationship is shown for both zero RF power input and an input power of 50 mW at 8.8 GHz. In accordance with the theoretical result, the dc resistance of the diode increases under the large-signal condition, and a decrease in current is observed above the threshold bias. Below the threshold, most of the crystal is biased in the linear ranges of the $v-E$ characteristic, and nonlinear effects are negligible.

Fig. 3 shows the CW current–voltage relationship for diode 1 when stabilized in the coaxial circuit. The 25-Ω impedance transformer was used. A decrease in current is again seen when 50-mW RF power is injected at 10 GHz.

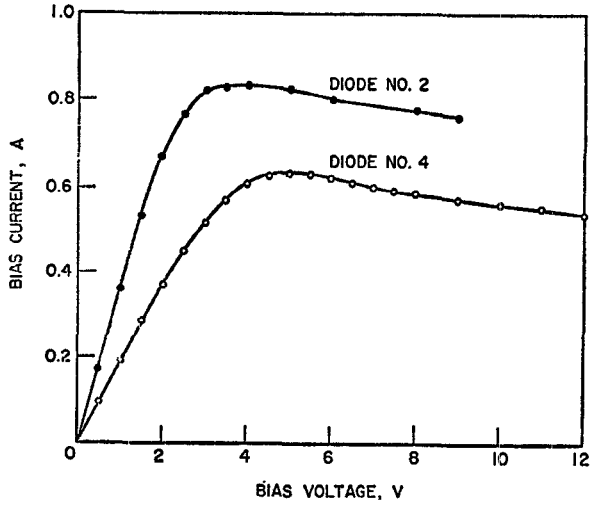

Fig. 4. CW current–voltage relationships for devices 2 and 4.

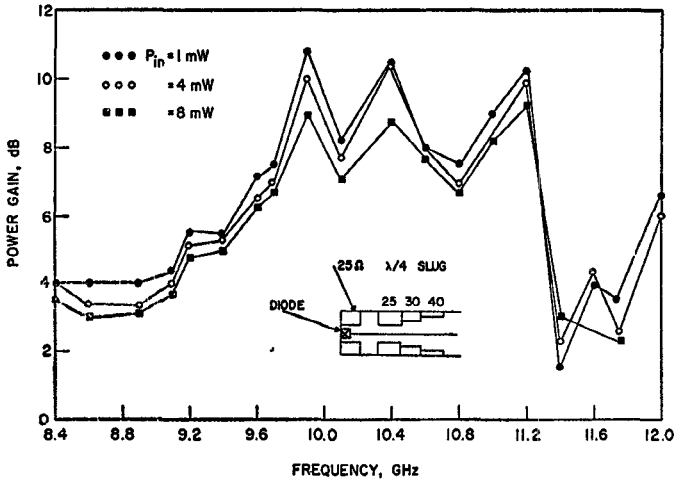

Fig. 5. Output power versus frequency for device 2 for different input powers. (Bias voltage = 9 V.)

CW current–voltage relationships for devices 2 and 4 are shown in Fig. 4.

B. RF Characteristics of Stabilized TE Amplifiers

One of the attractive features of TE amplifiers is their extremely wide bandwidth. Fig. 5 shows RF power gain as a function of frequency at different values of input power for device 2. The approximate circuit configuration is also shown in the figure. Gain is observed over a frequency band more than 3.6 GHz wide. A slight decrease in gain with an increase in RF power over most of the frequency band is seen. No gain expansion is observed except at 11.4 and 11.6 GHz because the signal strength is too large.

Measurements of output power as a function of frequency for an input power of approximately 3 mW are shown in Fig. 6 for device 3. The 10-Ω impedance transformer was used to obtain gain around 10 dB at bias values between 8 and 9.5 V. The maximum gain is seen to increase with bias voltage. This is because at relatively low bias, the negative resistance of the device increases with bias voltage, as predicted by theory. When it is considered that the length of the crystal of device 3 is 14 μm, gain occurs at somewhat high frequencies in Fig. 6. The transit-time frequency for a 14-μm device is approximately 7 GHz. However, theoretical calculations show that gain is expected at 10 GHz for relatively low bias voltages.

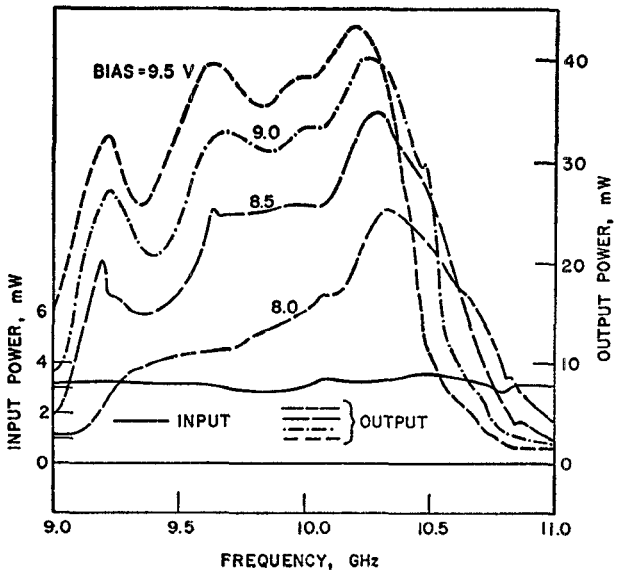

Fig. 6. Swept frequency measurement of output power versus frequency for different bias voltages. Device 3 with the 10-Ω impedance transformer placed at the diode end was used.

Theory predicts that the region of negative resistance occurs at lower frequencies with increase of bias voltage or lattice temperature. Fig. 6 exhibits this effect. By comparison of the experimental results with theoretical computation, it was found that most of the experimental change is due to the effects of increased lattice heating. The temperature increase lowers all electron velocities, and may be thought of as lowering the transit-time frequency.

In addition to the circuit, the device lead inductance and the package capacitance also affect the bandwidth of the amplifier. The magnitude of the reactance of these elements is of the same order as the device negative resistance and reactance. Thus the elements can introduce resonances within the frequency range of interest. For example, the lead inductance resonates in series with the device capacitance. At a higher frequency, the package capacitance resonates in parallel with the net inductance of the series combination of the crystal and the lead. At this frequency, the packaged device acts as a pure negative resistance, and the gain is maximum near this frequency. In general, these resonances decrease the $G^{1/2}B$ product (G = maximum power gain, B = 3-dB bandwidth) of these amplifier designs unless a special matching network is used. The $G^{1/2}B$ product for the data of Fig. 5 is approximately 5.4 GHz. In Fig. 6 it is approximately 5.2 GHz. It was much less when a single slug was used for tuning. Perlman *et al.* [1] have obtained $G^{1/2}B$ products of 8 GHz and larger by the use of microstrip circuits and equalizing networks.

It has been shown theoretically that as bias voltage is increased above threshold value, the magnitude of device negative resistance at first increases, reaches a maximum, and then decreases for fixed frequency. Thus in some circuits the device will exhibit stable amplification at a bias just above threshold, will oscillate as the bias is increased, and will become stable again at a higher bias. Such behavior has been observed by Perlman *et al.* [1]. However, if the magnitude of the maximum negative resistance is less than the positive resistance of the circuit, no oscillation occurs, and stable amplification is ob-

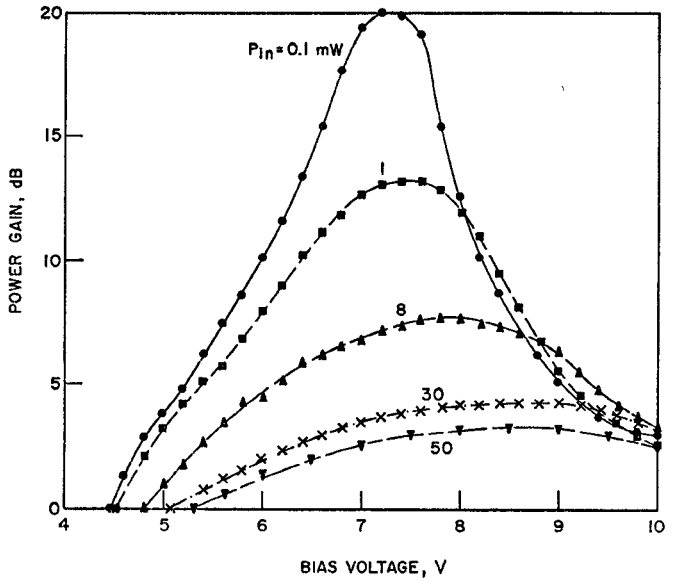

Fig. 7. Power gain versus bias voltage for device 1. The 25-Ω impedance transformer was used. (Frequency=9.75 GHz.)

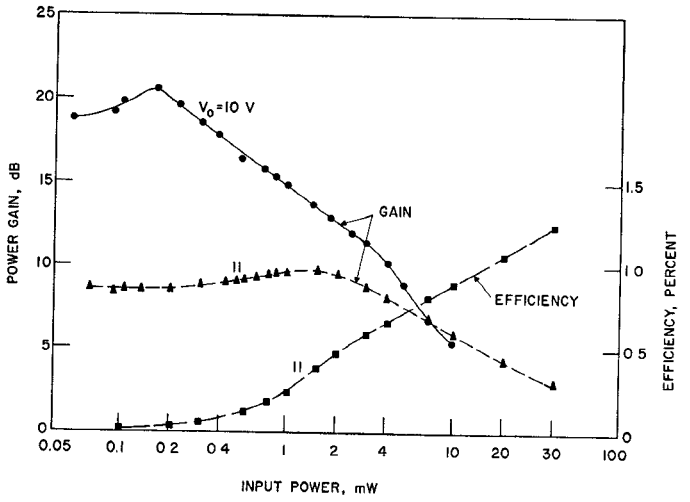

Fig. 8. Power gain and efficiency versus input power for device 1 with a λ/4 slug of characteristic impedance 25 Ω placed away from it. (Frequency=9.75 GHz.)

tainable over a wide range of bias values. In addition, the higher the RF input power, the higher is the bias voltage for which maximum negative resistance occurs. The minimum bias voltage at which the device exhibits negative resistance also increases with the input signal power.

Experimental data showing these effects are given in Fig. 7 where power gain is plotted as a function of bias voltage for constant RF input power levels for device 1. The signal frequency was 9.75 GHz and the 25-Ω impedance transformer was used at the device end of the circuit. The gain varies with bias as expected, and the minimum bias voltage at which gain is observed increases with signal strength. Also, in accordance with the theoretical results, the higher the signal power, the greater is the bias voltage at which maximum gain occurs.

It was shown theoretically that negative resistance increases as the RF signal is increased from a small value, reaches a maximum, and then decreases at large signals. This causes gain expansion, and it can be observed in the experi-

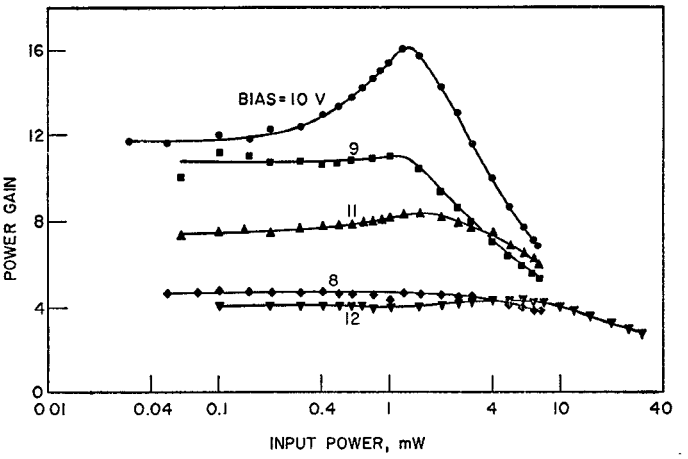

Fig. 9. Power gain versus input power for different bias voltages. Device 4 with a λ/4 slug of characteristic impedance 40 Ω placed away from it was used. (Frequency=9.42 GHz.)

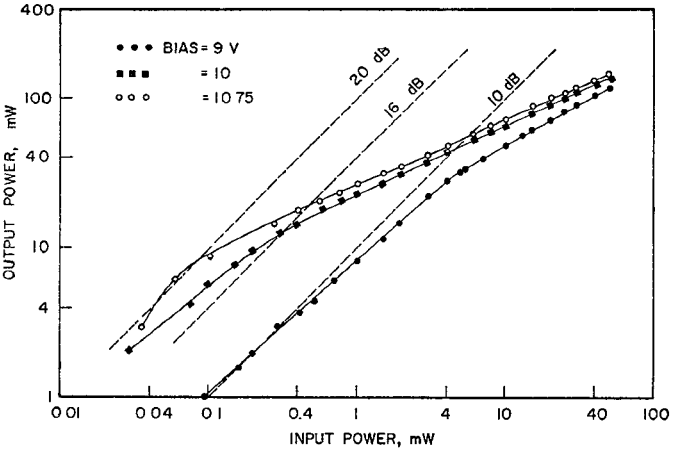

Fig. 10. Output power versus input power for device 3. The 25-Ω impedance transformer was used. (Frequency=8.8 GHz.)

mental data of Fig. 7 at bias voltages above 8 V. The gain expansion occurs at higher RF power input for larger values of bias voltage. This is shown more clearly in Fig. 8 for diode 1 where power gain is plotted as a function of input RF power for different bias voltage values. A single slug having a characteristic impedance of 25 Ω was used to obtain a maximum gain of approximately 20 dB at 10-V bias. The gain decreases at the higher bias of 11 V, and gain expansion occurs at a higher RF power level, as expected from the large-signal theory. The dc-to-RF conversion efficiency is also shown for the 11-V bias case.

Fig. 9 shows similar data for device 4. Here gain is plotted on a linear scale so that gain expansion can be more easily observed. As expected, gain increases with bias voltage for relatively low biases, and decreases when the bias is high. When the bias voltage is small and the difference between the magnitude of diode negative resistance and circuit resistance is large (so that gain is small), gain expansion may not be easily observable. This is the case at a bias of 8 V in Fig. 9. At higher bias voltages, gain expansion can be seen clearly. When the difference between the magnitude of device negative resistance and circuit resistance is small, the gain is large and is sensitive to change in the value of negative resistance. Such

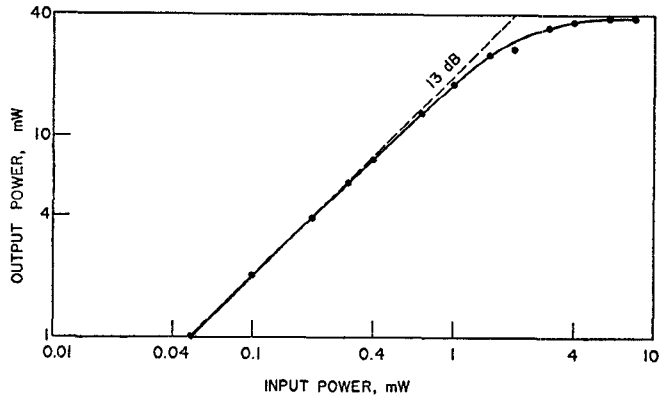

Fig. 11. Output power versus input power for device 5. The 10-Ω impedance transformer was used. (Frequency = 7.8 GHz, bias = 12.5 V.)

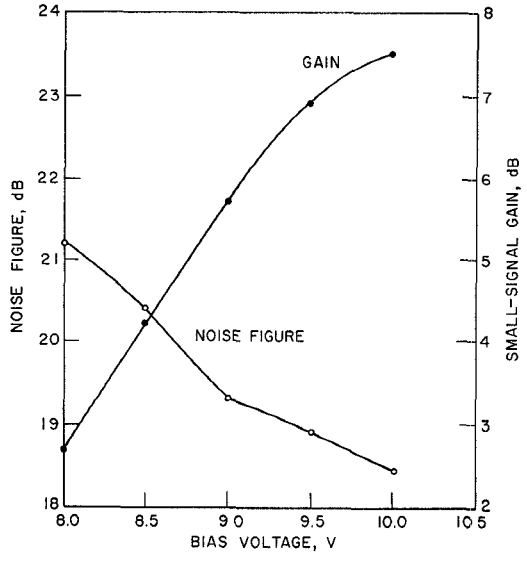

Fig. 12. Amplifier noise figure and gain for device 6 for a local oscillator frequency of 9.85 GHz and an IF frequency of 30 MHz.

a situation occurs at a bias of 10 V where gain expansion is substantial. Again, as predicted, gain expansion occurs at higher RF input power levels for higher bias voltages.

In general, the nonlinearity of the amplifier is higher at higher gains. Another example of such behavior is shown in Fig. 10 where RF power output is shown as a function of input power for device 3. Gain as well as nonlinearity increase here with bias voltage.

When the bias voltage is constant, the linearity of the amplifier depends on the circuit impedance at the signal frequency. For example, device 5 exhibited strong gain compression effects in one circuit, but in a different circuit showed fairly linear behavior, as seen in Fig. 11.

Fig. 12 shows the noise figure and gain measured as a function of bias voltage for device 6 in the coaxial circuit. The lowest noise figure measured was 18.4 dB at 9.85 GHz for 10-V bias and a gain of 7.5 dB. Standard noise measurement equipment was used with a 15.7-dB noise source for these tests. The amplifier 3-dB bandwidth at the given bias is 370 MHz. It is interesting to note that both the noise figure and noise measure decrease as bias voltage is increased.

Conclusion

Good qualitative agreement has been found between the experimental characteristics of stabilized transferred-electron amplifiers and the large-signal theoretical analysis. In particular, the following results have been verified.

1) Gain expansion, or the increase of gain with increase of RF signal power, occurs naturally as a large-signal effect. The higher the bias voltage, the higher is the RF power at which maximum gain occurs. Expansion effects can be minimized to give nearly linear gain over a wide range of input signal power.

2) RF power gain initially increases with increase of bias voltage, reaches a maximum, and then decreases with further increase of bias voltage. This occurs because the device negative resistance behaves similarly. Oscillation can occur near maximum gain if circuit loading is insufficient. The higher the RF input power, the higher is the voltage for maximum gain.

3) The frequency at which maximum gain is obtained decreases when the bias is increased, as well as when the lattice temperature increases. Therefore the choice of device thickness is not critical for a given frequency if bias voltage can be adjusted.

4) The bias current decreases strongly as lattice heating occurs. A current decrease above the usual threshold bias is directly caused by increased lattice temperature and not by domain formation in stabilized CW amplifiers. A current decrease also occurs for large RF signal power due to nonlinear effects.

5) Large gain-bandwidth products are realizable with simple circuits using stabilized transferred-electron devices.

Acknowledgment

The authors wish to thank J. T. Patterson for making the noise measurements and L. A. MacKenzie for supplying the devices used in this study.

References

[1] B. S. Perlman, C. L. Upadhyayula, and W. W. Siekanowicz, "Microwave properties and application of negative conductance transferred-electron devices," *Proc. IEEE*, vol. 59, pp. 1229–1237, Aug. 1971.

[2] J. Magarshack and A. Mircea, "Stabilized and wide-band amplification using over-critically doped transferred-electron diodes," in *Proc. 8th Int. Conf. Microwave and Optical Generation and Amplification*, Sept. 1970, pp. 16-19–16-23.

[3] A. A. Sweet and J. C. Collinet, "Multistage Gunn amplifiers for FM-CW systems," in *Proc. 1972 IEEE Int. Solid-State Circuits Conf. Dig.*, Feb. 1972, pp. 42–43.

[4] A. K. Talwar, "Theoretical and experimental investigations of transferred-electron amplifiers," Electron Phys. Lab., Univ. of Michigan, Ann Arbor, Tech. Rep. 127, Sept. 1972.

[5] A. K. Talwar and W. R. Curtice, "Effect of donor density and temperature on the performance of stabilized transferred-electron devices," *IEEE Trans. Electron Devices*, vol. ED-20, pp. 544–550, June 1973.

[6] ——, "A study of stabilized transferred-electron amplifiers," in *Proc. 3rd Biennial Cornell Elec. Eng. Conf.*, Aug. 1971, pp. 387–399.